

Segmentation of Solid Nodules in Ultrasonographic Breast Image Based on Wavelet Transform

Sangyun Park, Hyoun-Joong Kong, Woo Kyoung Moon, and Hee Chan Kim

Abstract—An accurate segmentation of solid nodules in ultrasonographic (US) breast image is presented. 1-level 2-dimensional Discrete Wavelet Transform (DWT) is used to create features reflecting the texture information of the original image. Using these features, the texture classification is achieved. Finally, solid nodule region is segmented from the classified texture region. Proper threshold for texture classification is automatically decided. Empirically acquired information about the relationship between the texture characteristic of the original image and the optimal threshold is examined and used. Presented algorithm is applied to 284 malignant solid nodules and 300 benign solid nodules and the resulting images are presented.

I. INTRODUCTION

BREAST cancer is one of the major causes of death for female in the world [1], [2] and is in an increasing trend. For the effective medication and treatment, Early detection of breast cancer is very important. Methods for early detection of breast cancer include biopsy, mammography and ultrasonography (US). Biopsy is the most accurate method for discrimination of breast cancer. However, biopsy is invasive, causing physical and psychological discomfort to patients. In addition to this drawback the negative-to-positive ratio of biopsy is very low; about 70%-90% of breast biopsies are performed in women with benign breast nodule [3], [4]. Therefore, mammography and US methods are expected to increase the negative-to-positive ratio of early diagnosis of breast cancer and to screen out the possibility of benign patients, resulting in an efficient biopsy. However, mammography uses x-ray and this can be harmful to the patient especially when frequently used. Because of this latent danger, mammography cannot be used very frequently. On the other side, US is safe but the image quality of US is not as good as that of mammography.

Therefore, the image processing technique for US needs to

Manuscript received April 16, 2007. This work was supported by Grant No. R01-2006-000-10717-0 and grant No. R01-2005-000-10875-0 from the Basic Research Program of the Korea Science & Engineering Foundation.

Sangyun Park is with Interdisciplinary Program, Biomedical Engineering Major, Graduate School, Seoul National University, Seoul, Korea (email: pinkydays@melab.snu.ac.kr).

Hyoun-Joong Kong is with Interdisciplinary Program, Biomedical Engineering Major, Graduate School, Seoul National University, Seoul, Korea (email: gongcop@melab.snu.ac.kr).

Woo Kyoung Moon is with the Department of Radiology, Seoul National University, Seoul 110-744, Korea. (moonwk@radcom.snu.ac.kr).

Hee Chan Kim is with Department of Biomedical Engineering, College of Medicine and Institute of Medical and Biological Engineering, Medical Research Center, Seoul National University, Seoul, Korea (email:hckim@snu.ac.kr).

be improved. Especially, the fact that the characteristics of benign and malignant lesion in US image can be overlapped considerably can be a serious problem [5]. Many researchers have studied to solve this problem. Stavros *et al.* reported an US image classification algorithm using 20 features with significantly high performance [6]. But subsequent studies showed that there were difficulties in identifying specific US features [3], [7]. Chen *et al.* [8] and Joo *et al.* [3] reported artificial neural network (ANN) based computer-aided diagnosis (CAD) systems. These researches attracted attention in that their methods targeted an automatic classification system. In the case of Joo's research, although the morphological shape of the solid nodule is one of the most important features, the nodule segmentation algorithm is not accurate enough, especially for the malignant nodule in US image.

In this study, we segmented solid nodule lesion by the texture information in US breast image. To achieve texture information from the original image, a 2-dimensional Discrete Wavelet Transform (DWT) algorithm was used. DWT decomposes original image into the lower sub-band and higher sub-bands (Fig. 1.), (Fig. 3.). This information about both frequency and space domain can be very useful in taking features that reflect texture characteristics.

II. MATERIAL AND METHODS

The US images were provided by the Seoul National University Hospital, Seoul, Korea. The database was composed of 284 malignant and 300 benign images. The prospectively collected images were a consecutive series of solid masses seen at US and confirmed histologically. US was performed by one breast radiologist by using a HDI 3000 (Advanced Technology Laboratories, Bothell, WA) or a Voluson 730D (GE Medical Systems, Milwaukee, WI) machine with a 10-MHz transducer and freeze-frame capability. A 640×480 digital image was captured from the US scanner, where 1 pixel size corresponds to $0.11\text{mm} \times 0.11\text{mm}$.

Our method for breast nodule segmentation consists of four steps (Fig. 2.).

First, we find 4 features for each pixel in the original image. In this feature extraction step, the 1-level 2-dimensional DWT is used to reflect the texture information to the 4 features.

Second, from the information described above, we

determine the inter class distance threshold value. Empirically collected data are used to optimize the threshold value to make a decision rule.

Third, Texture classification is achieved by the algorithm which will be presented later.

Fourth, Classified region is smoothed and segmentation is finished.

The second step is for deciding proper threshold value for the classification algorithm. This step is explained after the third step for the reader's effective comprehension.

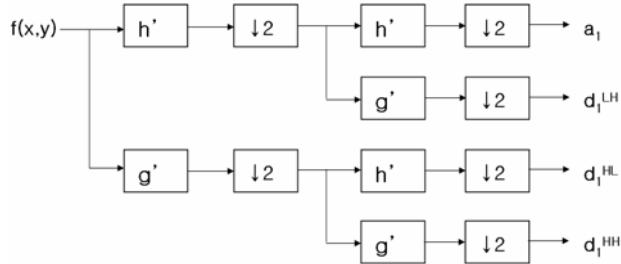


Fig. 1. Schematic of 1-level DWT. a_1 is the coefficient of lower frequency element. d_1^{LH} : higher and horizontal, d_1^{HL} : higher and vertical, d_1^{HH} : higher and diagonal.

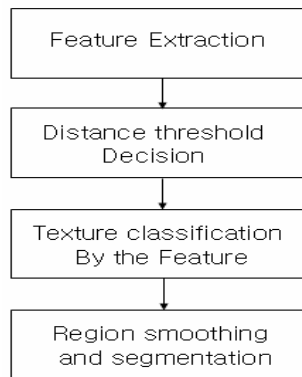


Fig. 2. Schematic of the breast nodule segmentation algorithm

A. Feature Extraction by 2-Discrete Wavelet Transform

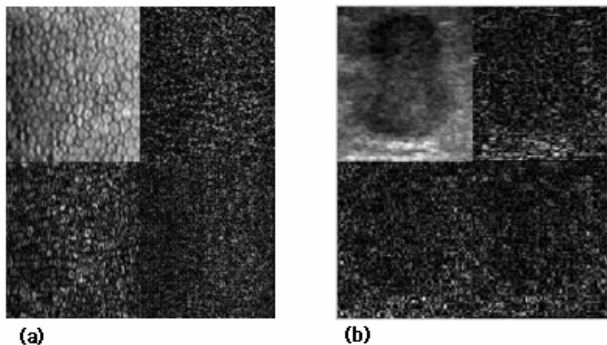


Fig. 3. 4 sub-bands in 1-level DWT decomposition of the cell image (a) and the breast nodule sonogram image (b)

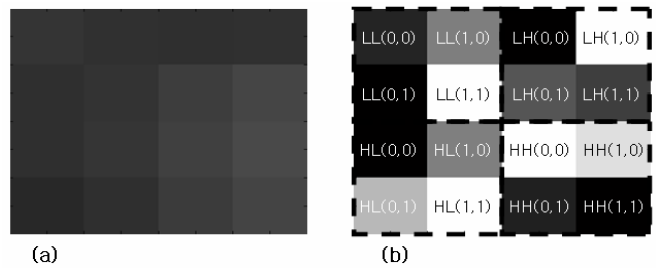


Fig. 4. 4*4 original image block (a) and 4 sub-bands in 1-level DWT decomposition of the original image block (b). Each 4 pixels in a box of dotted lines are LL, LH, HL and HH sub-band.

The proposed algorithm allocates 4 features for each pixel of the original image in a 4 by 4 sized window sliding. Image block of 4 by 4 pixels is decomposed by the 1-level 2-d DWT algorithm into the 4 sub-bands. Let these 4 sub-bands be denoted as LL, LH, HL and HH bands. Each sub-band has 4 coefficients and we use these coefficients to evaluate the energy of each sub-band (Fig. 4.).

For example, the 4 coefficients in the LL sub-band are $\{C_{LL}^{(0,0)}, C_{LL}^{(0,1)}, C_{LL}^{(1,0)}, C_{LL}^{(1,1)}\}$ and the feature from the LL sub-band is

$$F_{LL} = \sum_{i=0}^1 \sum_{j=0}^1 C_{LL}^2(i,j) / 4.$$

So each pixel has 4 features: F_{LL}, F_{LH}, F_{HL} and F_{HH} . Ying Liu *et al.* [9] demonstrated texture feature of the image by DWT algorithm in a similar way, but they used a block-wise operation instead of window sliding. Because their study is about image retrieval, the response time was more important than the exact boundary segmentation. In our US solid nodule segmentation, fine boundary extraction is important, so we used the sliding window method. As a result, in the algorithm of Ying Liu *et al.* 4 features are allocated for each 4 by 4 block, where in our algorithm 4 features are allocated for each pixel.

B. Texture classification by the feature

The first pixel to be classified is assumed to be the element of the first class. From the second to the last pixel, each pixel either gets included into the existing class or allocated to a new class and becomes the first element of the created class as the first pixel did. Each pth class has its 4 features: $f_{LLp}, f_{LHp}, f_{HLp}$ and f_{HHp} . When there are p classes and the new pixel with feature $(F_{LL}, F_{LH}, F_{HL}, F_{HH})$ comes, distances between the new pixel and the existing classes are calculated. The distance between a pixel with features $(F_{LL}, F_{LH}, F_{HL}, F_{HH})$ and the lth class which has the features $(f_{LL}^l, f_{LH}^l, f_{HL}^l, f_{HH}^l)$ is defined as:

$$D_l = \sum_{i=LL}^{HH} \sqrt{(F_i - f_i^l)^2}$$

The minimum distance is defined as:

$$\min(D_l)_{l \in L}, L = \{1, \dots, p\}$$

When the minimum distance is bigger than the threshold, the p+1th class is created and the new pixel becomes the first element of the p+1th class. The p+1th class has feature $(f_{LL}^{p+1}, f_{LH}^{p+1}, f_{HL}^{p+1}, f_{HH}^{p+1})$ which is the same as the first element pixel feature $(F_{LL}, F_{LH}, F_{HL}, F_{HH})$.

When the minimum distance is smaller than the threshold, the new pixel with feature $(F_{LL}, F_{LH}, F_{HL}, F_{HH})$ is included into the jth class where the distance $(D_l)_{l \in L}, L = \{1, \dots, p\}$ between the class and the new pixel is minimum. When the jth class had(x) has k elements, the feature of the class $(f_{LL}^j, f_{LH}^j, f_{HL}^j, f_{HH}^j)$ is updated as:

$$\left[(f_q^j)_{new} = \frac{k \times (f_q^j)_{old} + F_q}{k+1} \right]_{q \in \{LL, LH, HL, HH\}}$$

In addition, the proposed algorithm for classification does not scan in the *top-left to bottom-right* manner. Instead of such, when the algorithm starts all of the pixels are randomly ordered so that the classification order becomes random. Empirically we found that this random classification is better than raster scanned windowing.

C. Decision of the inter class distance threshold

The proposed classification algorithm needs inter-class distance threshold. According to the presented algorithm, as the threshold gets smaller the number of classes gets bigger. Proper threshold value should be proposed to make proper numbers of classes and to achieve precise segmentation. Empirically we found that the proper number of classes is about 10.

All $M_0 \times N_0$ pixels in original image have their pixel features:

$$(F_{LL}^{(i,j)}, F_{LH}^{(i,j)}, F_{HL}^{(i,j)}, F_{HH}^{(i,j)})_{(i,j) \in \{(1,1), (1,2), \dots, (M_0, N_0)\}}$$

And we proposed 4 indices reflecting the image character which is from the pixel features:

$$\left[std(F_p) = \left[\frac{\sum_{i=1}^{M_0} \sum_{j=1}^{N_0} F_p^{(i,j)}}{M_0 N_0} \right]^2 \times \frac{1}{M_0 N_0} \right]_{p \in \{LL, LH, HL, HH\}}$$

These 4 indices are the standard deviation of the 4 feature values at the each $M_0 \times N_0$ points of original image. To

evaluate the texture characteristic of the original image we examined many statistical values of these 4 indices:

$$(std(F_{LL}), std(F_{LH}), std(F_{HL}), std(F_{HH}))$$

We concluded that the simple average of 4 indices is the optimal statistical value which represents the texture information of the original image.

If we let the average of 4 indices be denoted as *mean deviation of features*, we found correlation between the mean deviation of features and the empirically estimated proper threshold for image segmentation (Fig. 5).

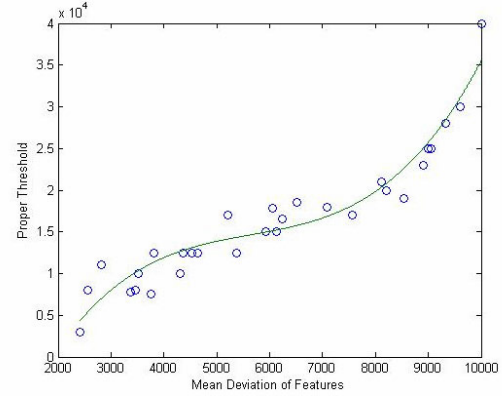


Fig. 5. Mean Deviation of Features Vs Proper Threshold found to have correlation. With the 31 empirical data points, we get polynomial curve of order 3.

D. Region smoothing and segmentation from the classes

Randomly ordered classes are properly ordered by the first element of the class of the elements in classes, we decide which class region is the feature f_{LL} because the first element represents lower sub-band energy, in other words, pseudo-intensity of the class. From the first element of the class feature and the number of the elements in classes, we decide which class region in the nodule region. Finally, region contour is smoothed and the nodule region is segmented.

III. RESULT

284 malignant images and 300 benign images were examined. For all the images, region of interest (ROI) was detected and cropped before the experiment. Generally the malignant image segmentation showed better result.

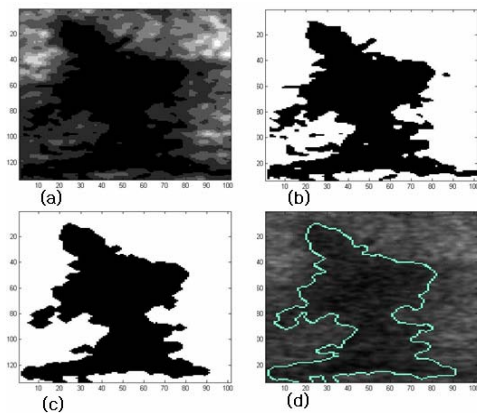


Fig. 5. (a) Texture classification. (b) Nodule class extracted. (c) Contour of the Nodule class is smoothed. (d) Original image nodule region segmentation finished. Original image is from malignant nodule.

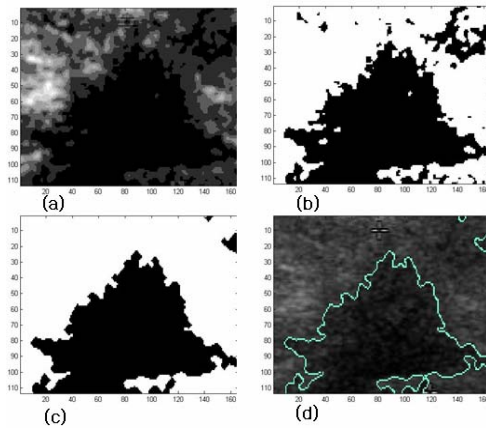


Fig. 6. (a) Texture classification. (b) Nodule class extracted. (c) Contour of the Nodule class is smoothed. (d) Original image nodule region segmentation finished. Original image is from malignant nodule.

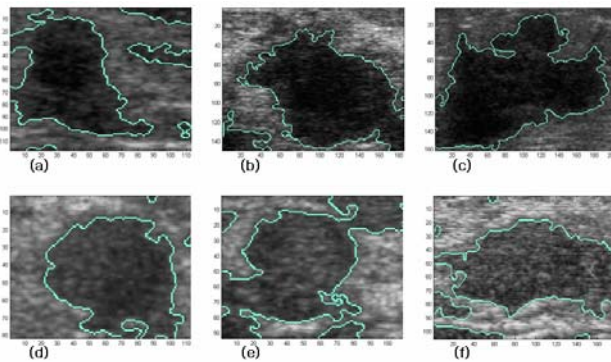


Fig. 7. Segmentation of malignant nodules (a) (b) (c) and malignant nodules (d) (e) (f) are segmented in good manner.

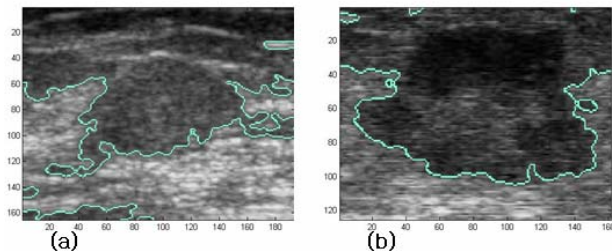


Fig. 8. Segmentation of malignant nodule (a) and Segmentation of malignant nodule (b) is not so good.

In the texture classification step, 6 images from 300 benign solid nodule images were classified as just one class, which means that the texture classification algorithm was entirely malfunctioned. This phenomenon could be caused by the fact that the threshold was decided by the information from the malignant images. But the general performance of the algorithm was applicable.

IV. DISCUSSION

US is one of the promising technology for early detection of breast cancer. For malignant and benign solid nodule classification, morphological segmentation of solid nodule is very important. We segmented solid nodules by the texture classification method and 2d DWT was used to gather texture information of the original image. Both malignant and benign solid nodules are successfully segmented at most times. But still the failure of segmentation is observed. Fine segmentation of solid nodule can provide more reliable morphological information of solid nodule. With this morphological information, malignant and benign solid nodule classification could be achieved and the subgroups of malignant nodules could be classified.

REFERENCES

- [1] Boring CC, Squires TS, Tong T. Cancer statistics 1993. CA: CancerJ. Clinicians, vol. 43, pp. 7-26, 1993.
- [2] Wingo PA, Tong T, Bolden S. Cancer statistics 1995. CA: CancerJ. Clinicians, vol. 45, pp. 8-30, 1995.
- [3] Segyoung Joo, Yoon Seok Yang, Woo Kyoung Moon, and Hee Chan Kim, "Computer-Aided Diagnosis of Solid Breast Nodules: Use of an Artificial Neural Network Based on Multiple Sonographic Features", IEEE Transactions on Medical Imaging, Vol. 23, No. 10, pp. 1292-1300, October 2004
- [4] J. E. Meyer, T. J. Eberlein, P. C. Stomper, and M. R. Sonnenfeld, "Biopsy of occult breast lesions: Analysis of 1261 abnormalities," J. Amer. Med. Assoc., vol. 263, pp. 2341-2343, 1990.
- [5] G. Rahbar, A. C. Sie, G. C. Hansen, J. S. Prince, M. L. Melany, H. E. Reynolds, V. P. Jackson, J.W. Sayre, and L.W. Bassett, "Benign versus malignant solid breast masses: US differentiation," Radiology, vol. 213, pp. 889-894, 1999.
- [6] A. T. Stavros, D. Thickman, C. L. Rapp, M. A. Dennis, S. H. Parker, and G. A. Sisney, "Solid breast nodules: Use of sonography to distinguish between benign and malignant lesions," Radiology, vol. 196, pp.123-134, 1995.
- [7] J. A. Baker, P. J. Kornguth, M. S. Soo, R. Walsh, and P. Mengoni, "Sonography of solid breast lesions: Observer variability of lesion description and assessment," Amer. J. Roentgenol., vol. 172, pp.1621-1625, 1999.
- [8] D. R. Chen, R. F. Chang, and Y. L. Huang, "Computer-aided diagnosis applied to US of solid breast nodules by using neural networks," Radiology, vol. 213, pp. 407-412, 1999.
- [9] Liu, Ying; Wu, Si; Zhou, Xiaofang, "Texture segmentation based on features in wavelet domain for image retrieval," Proceedings of SPIE , Vol. 5150, June 2003, pp. 2026-2034